Drug Delivery and Translational Research (2019) 9:394–403
https://doi.org/10.1007/s13346-018-0579-4

METHODS PAPER

The synthesized transporter K16APoE enabled the therapeutic HAYED peptide to cross the blood-brain barrier and remove excess iron and radicals in the brain, thus easing Alzheimer's disease

Zhenyou Zou[1,2] · Qiqiong Shen[1] · Yanxia Pang[3] · Xin Li[1] · Yongfeng Chen[1] · Xinjuan Wang[1] · Xinhua Luo[4] · Zhongmin Wu[1] · Zhaosheng Bao[1] · Juanli Zhang[1] · Jiawei Liang[1] · Lingjia Kong[1] · Lunan Yan[1] · Lijun Xiong[1] · Tianjun Zhu[1] · Shuaibin Yuan[1] · Miaoyang Wang[1] · Kewei Cai[1] · Yinning Yao[1] · Jianchao Wu[1] · Yuding Jiang[1] · Heng Liu[1] · Jing Liu[1] · Yan Zhou[1] · Qianqian Dong[1] · Wei Wang[1] · Kangjie Zhu[1] · Li Li[5] · Yingjie Lou[1] · Hongdian Wang[1] · Yizi Li[1] · Hong Lin[1]

Published online: 22 August 2018

Abstract

Alzheimer's disease (AD) is currently incurable and places a large burden on the caregivers of AD patients. In the AD brain, iron is abundant, catalyzing free radicals and impairing neurons. The blood-brain barrier hampers antidementia drug delivery via circulation to the brain, which limits the therapeutic effects of drugs. Here, according to the method described by Gobinda, we synthesized a 16 lysine (K) residue-linked low-density lipoprotein receptor-related protein (LRP)-binding amino acid segment of apolipoprotein E (K16APoE). By mixing this protein with our designed therapeutic peptide HAYED, we successfully transported HAYED into an AD model mouse brain, and the peptide scavenged excess iron and radicals and decreased the necrosis of neurons, thus easing AD.

Keywords Alzheimer's disease · Iron · Radical · Blood-brain barrier · K16APoE · HAYED peptide

Introduction

Alzheimer's disease (AD) is a progressive neurodegenerative disease characterized by memory and cognitive decline [1]. AD is currently incurable and places a large burden on the caregivers of patients [2].

The cause of AD is not well understood. Increased oxidative radicals in the brain have been reported to have a pathogenic role in the development of AD; they impair membrane lipids and proteins, ultimately resulting in neuronal death [3, 4].

Iron is a transitional metal that catalyzes free oxidative radical generation by deoxidizing oxygen to oxyradicals or by donating electron to hydrogen peroxide, forming hydroxyl radicals [5]. Previously, we revealed that AD brains have higher iron levels than do normal brains, and the iron distribution determines the regional density of radicals [6]. Therefore, reducing the redundant iron in the brain may be an option to ease AD.

Desferrioxamine (DFO) and deferiprone (DFP) have been used as metal chelators to treat AD in clinical trials [7]. These agents have slowed the progression of AD in certain cases [8,

Zhenyou Zou, Qiqiong Shen, Yanxia Pang and Xinhua Luo contributed equally to this work.

✉ Zhenyou Zou
sokuren@163.com

✉ Xinhua Luo
luoxiangnanchang84@163.com

✉ Li Li
l.li@nki.nl

[1] Medical College of Taizhou University, Taizhou 318000, China

[2] Biochemistry Department of Purdue University, West Lafayette, IN 47906, USA

[3] Shanghai Key Laboratory of Forensic Medicine, Shanghai Forensic Service Platform, Academy of Forensic Science, Shanghai 200063, China

[4] Clinic Laboratory of Taizhou Municipal Hospital, Taizhou 318000, China

[5] Oncogenomics Division of Netherlands Cancer Institute, 1066 CX Amsterdam, Netherlands

9]; however, fundamental aspects of their biochemistry have severely limited their effectiveness. For example, the hexadentate iron chelator DFO can tightly bind iron (III) to impede the progression of AD [10–12]; the lipid-soluble iron chelator DFP can lower neutrophils and white blood cell counts, causing life-threatening infections [13, 14]. Therefore, seeking nontoxic iron chelators that remove excess iron from the brain is a pressing concern.

The amyloid beta (Aβ) peptide was reported to have high affinity to Cu^{2+} and Fe^{3+}, as it can bind excess iron ions at sites Asp $(D)_1$, Glu $(E)_3$, and His $(H)_{6,13,14}$, thus enabling it to reduce the excess free iron in CSF [15–18]. However, due to the low solubility and potential malignant activity in the radical catalyzing of the Aβ peptide, we deleted the nonpolar residues and combined the metal-pro amino acid Asp (D), Glu (E), and His (H) residues, the polar amino acid tyrosine (Y) and the smallest nonpolar amino acid alanine (A) to form a new amino acid oligomer. We tried delivering this oligomer to the CSF by way of intravascular injection with the aim of chelating excess iron and decreasing radicals in the brain, thus easing AD.

However, before the oligomer flowed into the cerebrospinal fluid, the blood-brain barrier (BBB), formed by the tight junctions of endothelial cells in vessel walls, severely hampered the transmission [19]. Varied methods have been sought to transport drugs across the blood-brain barrier. In response to the insufficiency in conventional delivery mechanisms, intracerebro-ventricular infusion, CNS drug releasing microchip implantation, pluronic micelles incorporation, and liposome capsule had been utilized to deliver the therapeutic drugs to the brain. As an example, Pardridge et al. constructed a kind of Trojan Horses Liposomes (THL) which successfully delivered a shRNA crossing BBB-treated Parkinson's disease (PD) in rat model. Transporters and receptors are essential for recognizing or transporting nutrient or hormones to the body for the metabolism and survival. They, which expressed at the BBB, had also been exploited to deliver drugs into the brain. A large neutral amino acid carrier had been reported used to deliver L-Dopa to patients with Parkinson's disease, resulting in clear clinical benefit [20–23].

Low-density lipoprotein receptor-related protein (LRP) is a category of receptor that mediates the endocytosis of multiple ligands and cleaves the signal segment on the ligand after entry expressed on the BBB [23, 24]; Gobinda used LRP-binding amino acid segments of apolipoprotein E (151–170, Swiss-Prot # P02649)-linked 16 lysine (K) residues to form a non-covalent transport K16ApoE, which successfully delivered beta-galactosidase, IgG, and IgM to the brain [19].

According to the method described by Gobinda in his article, we also synthesized K16ApoE and used it to deliver our therapeutic HAYED oligomers across the BBB in the AD brain. To verify the effectiveness of our products, we administered them to the AD model Kunming (KM) mouse. These mice display symptoms similar to those displayed by human patients with AD, such as memory deterioration, neurofibrillary tangles, gliocyte hyperplasia, and inflammation; in particular, brain iron levels are higher in these mice than in normal mice [25], which is quite suitable for examining brain radical levels and damage as well as for performing cognitive assays after drug administration. Specifically, we mixed HAYED peptides with K16ApoE and then injected the compounds by cardiac injection into the AD mice and let them spread via circulation. Using immunohistochemistry, we verified that HAYED crossed the BBB and entered the brain to scavenge iron and radicals with the help of K16ApoE. Using a TUNEL assay, we demonstrated that the HAYED peptide functioned in a neuron-protecting role. Furthermore, by using functional nuclear magnetic resonance (fMRI) and the Morris water maze, we found that HAYED ameliorated cognitive decline in AD mice.

Results

Identification of the transport K16APoE and the therapeutic peptide HAYED

The transporter K16APoE and the therapeutic amino acid oligomer HAYED were synthesized. Figure 1a, b shows the mass spectra of these proteins. In Fig. 1a, the particles with 6 hydrions appeared at 825.66, 5 hydrion particles were located at 990.58, and 4 hydrion participles peaked at 1238.16. The molecular weight of the entire peptide was 4953.96, and the sequence was "LRVR LASH LRKL RKRL LRDA KKKK KKKK KKKK KKKK" as assayed by a protein sequencer. Furthermore, 715.85 was the position of 5 hydrion particles, a peak of 894.3 was the signal of 4 hydrion particles and 1192 for 3 hydrion particles. The total molecular weight was 3574.5, which was the exact weight of 5 repeats of the HAYED oligomer. The sequencer identified the repeats as "HAYED HAYED HAYED HAYED HAYED" in sequence.

The synthesized HAYED peptide can bind iron

Fig. 2a (c and d) show the TEM images of the HAYED oligomers before and after $FeCl_3$ incubation. Without $FeCl_3$, the oligomers displayed liner-like fibrils, and the bright spots, representing the Fe positions (right panel of Fig. 2a (c), detected by the X-ray energy spectrometer), were scarce and randomly scattered. In contrast, after $FeCl_3$ treatment, the oligomers curled and conglomerated (Fig. 2a (d), and the iron was co-distributed and iso-directed along the fibrils (right panel of Fig. 2a (d), which strongly suggests that iron atoms bind to the amino acid oligomer.

ITC revealed that HAYED has an affinity to iron. As shown in Fig. 2b (b), after the $FeCl_3$ titration, HAYED lost

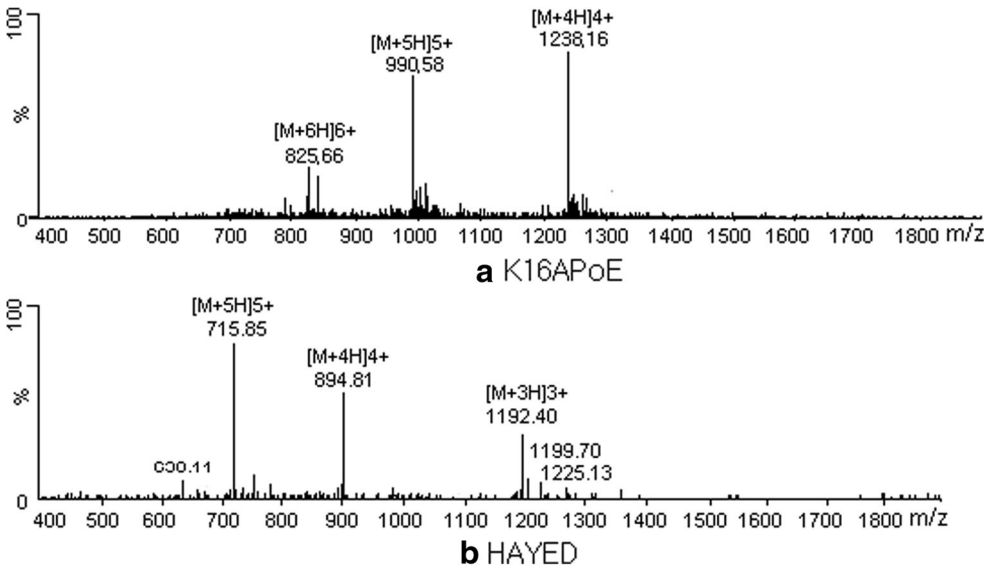

Fig. 1 Mass spectra of K16APoE and HAYED amino acid oligomers. **a** Mass spectrum of K16APoE; the particle with 6 hydrions appeared at a peak of 825.66, 5 hydrion particles were located at 990.58, and 4 hydrion particles at 1238.16. The molecular weight of the whole peptide was 4953.96 D. **b** MS of HAYED: peak 715.85 was the 5 hydrion particles; peak 894.3 was the 4 hydrion particles, and 1192 was the peak of 3 hydrion particles. The weight of the whole molecule was 3574.5 D, exactly the weight of 5 repeats of the HAYED oligomer

77,253 kCal/mol in enthalpy and 8210.6 kCal/mol in Gibbs. In contrast, when titrated with ITC buffer, no binding to HAYED occurred (Fig. 2b (a)).

Infrared chromatography further indicated that the HAYED oligomer bound iron at residues His, Tyr, Asp, and Glu. The peaks in the band of 1600–1300 cm^{-1}, which represent the C = O group vibration in the carboxyl of Glu and Asp, changed after incubation with $FeCl_3$; the peak 1018.21 cm^{-1} shifted to 873 cm^{-1} and weakened, representing the change in the phenyl hydroxide of Tyr (Fig. 2c (b)). The absorption apex at 2385.95 cm^{-1}, which represented the stretching of the C-N bond, redshifted to 2349.30 cm^{-1}; the peaks in the 1700–1615 cm^{-1} band, which displayed the stretching of the C = N bond in the imidazole ring of the histidine residue, were all weakened (Fig. 2c (b)), suggesting that iron chelating occurred on these residues.

HAYED can protect cells by reducing iron and the catalyzed radicals

To understand the efficiency of synthesized HAYED on the rescue of iron-stressed cells, we administered the peptide to the iron-rich medium (containing 0.016 M $FeCl_3 \cdot 6H_2O$, imitating AD cerebrospinal fluid) and the cultured SH-sy5y cells. As shown in Fig. 3a (a, b), after 36 h of iron stress, more than 50% of the cells died. However, when 100 pM HAYED was pre-added to the high iron-containing medium, more than 80% of the cells survived, suggesting that HAYED protected the cells.

ICP and spectrophotometry assays revealed that the HAYED peptide cleared the redundant iron and hydroxyl radicals in the medium (Fig. 3c, d). The free iron in the medium was decreased by 50%, and the hydroxyl radical was decreased by 62% in terms of the OD value.

The synthesized K16APOE can help HAYED cross the BBB to enter the brain

After labeling the brain with the prepared immune serum, the brain that had the pre-injected HAYED-K16APoE mixture was stained brown (Fig. 4a (d)), whereas the brain treated with HAYED alone was not stained (Fig. 4a (b)), suggesting that K16APoE enabled HAYED to enter the brain. ^{3}H-autoradiography demonstrated that more than 30% HAYED entering the brain or retained the activity. As Fig. 4b (b) shown, 2 days after the cardiac injection of 200 μl 1.25 μM ^{3}H-HAYED-K16APoE mixture, the concentration of the remnant ^{3}H-HAYED in the brain was about 0.3 μM, which being still active.

K16APoE carried HAYED across the BBB, entering the brain and thus reducing iron and radicals and bringing about neuronal protection

As shown in Fig. 5a (d), b, c, when HAYED was not mixed with K16APoE, the iron, radicals and necrotic neurons in the brain remained as high as those in the AD mouse, suggesting that HAYED did not enter the brain to function in the role of neuronal protection. In contrast, if HAYED was mixed with K16APoE, HAYED was detected in the brain (Fig. 4a (d)), and the iron and hydroxyl radicals decreased (Fig. 5b, c). The number of necrotic neurons was also reduced (Fig. 5a (b)), suggesting that K16APoE helped therapeutic HAYED enter the brain and protect neurons.

HAYED can ameliorate the cognitive status of AD mice

After 1 month of weekly cardiac injection of the HAYED-K16APoE mixture, by using fMRI, we found that the blood

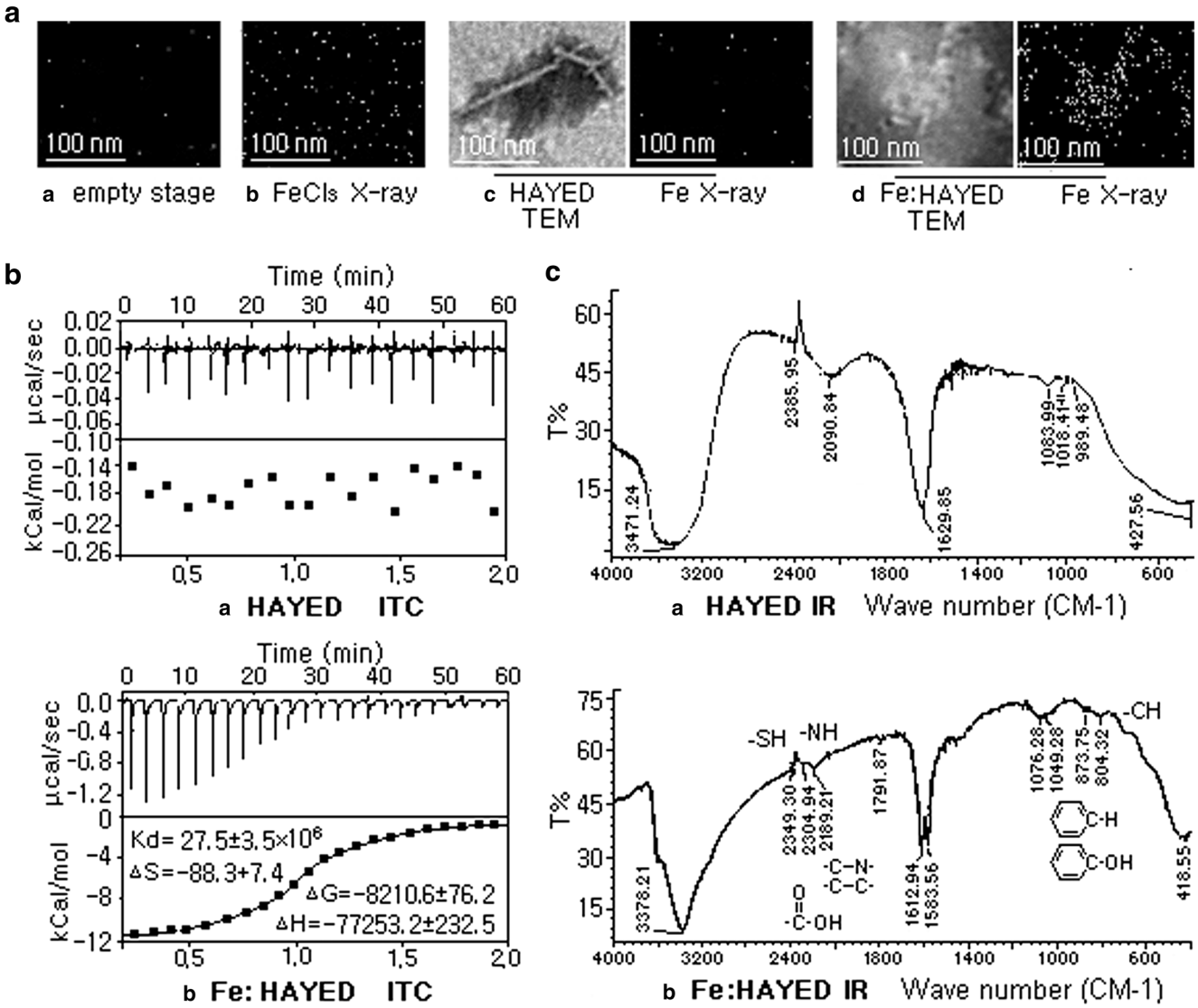

Fig. 2 HAYED oligomer can bind iron ions. **a** TEM image of HAYED oligomers with or without the $FeCl_3$ incubation and Fe distribution detected by X-ray energy spectrum. The $FeCl_3$ incubation resulted in the agglomeration of the HAYED oligomer, and iron was iso-directed along the amino acid fibril. **b** Isothermal titration calorimetry showing that the enthalpy of the Fe: HAYED compound lost 77,253 kCal/mol enthalpy and 8210.6 kCal/mol Gibbs, indicating that HAYED has a higher affinity to iron. **c** Infrared spectra of HAYED before and after $FeCl_3$ incubation. The signals of phenyl-OH (873 cm^{-1}) in the Tyr residue, -COOH (2925 cm^{-1} and 1600~1300 cm^{-1}) in the Glu and Asp residues, and C-N (2349.30 cm^{-1}) and C = N (700~1615 cm^{-1}) in the His residue were weakened, suggesting iron binding. Furthermore, the signals representing the backbone acylamide N-H stretching (3500~3100 cm^{-1}), the C = O bond shift (1680~1630 cm^{-1}), the N-H bending (1655~1590 cm^{-1}), and C-N stretching (1420~1400 cm^{-1}) were transformed, indicating that a tortuosity occurred in the backbone after the iron incubation. $N = 5$; $^{*}p < 0.05$

oxygen metabolism level (bright areas in the brain shown in Fig. 6a) in the AD mouse brain increased by 152% on average compared with the wild-type AD mice. In the AD mice treated with HAYED alone (Fig. 6a (c)), the blood oxygen metabolism level was only 32% of that in normal mice and was nearly the same level as that in AD brains. The injected HAYED did not take effect in the absence of K16APoE.

In addition, the Morris water maze assay disclosed that after 4 days of learning, the HAYED-K16APoE mixture-treated mice were less clumsy than the untreated wild-type aged AD mice and the HAYED-only treated AD mice. These mice spent 59 s on average to return to the platform, nearly 23 s less than the untreated mice and 19 s less than the HAYED-only treated AD mice (Fig. 6c). Therefore, K16APoE helped HAYED significantly improve the cognition status of the AD mice.

Discussion

Alzheimer's disease is characterized by abundant amounts of iron in CSF, which catalyzes radicals and impairs neurons, resulting in neurodegeneration [6, 26]. Removal of

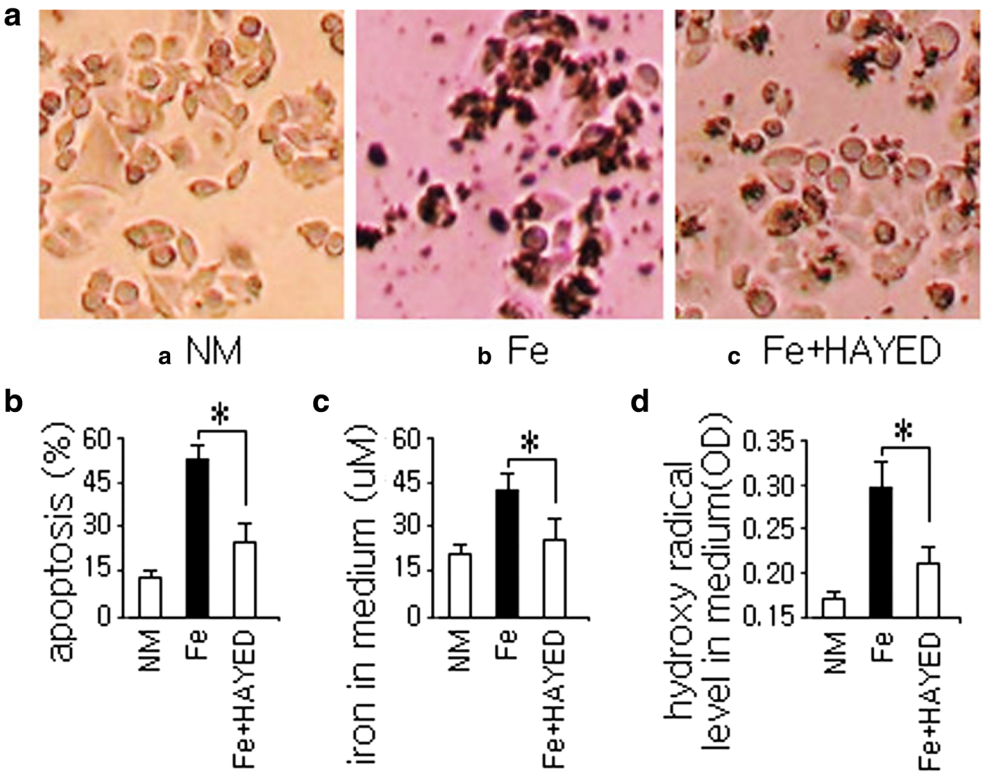

Fig. 3 HAYED can reduce redundant iron and hydroxyl radicals that protect cells. **a**, **b** Approximately 50% of SH-sy5y cells were dead after 36 h of iron-rich medium culture; in contrast, if the high-iron medium was supplemented with HAYED, more than 80% of the cells survived. **c**, **d** HAYED peptide reduced hydroxyl radicals and free iron in the medium, resulting in increased cell survival. $N = 5$; $^*p < 0.05$

excess brain iron may be a potential therapy for AD. Desferrioxamine (DFO) and deferiprone (DFP) have been used as agents to chelate the excess metal and treat AD in clinical trials [7]. These drugs have slowed the progression of AD in certain cases [8, 9]; however, their biochemical characteristics have severely limited their effectiveness, as DFO can tightly bind iron (III) to impede the progression of AD [10–12], and DFP can cause life-threatening infections [13, 14]. Therefore, identifying other nontoxic scavengers to remove excess iron from the brain is needed.

The amyloid beta (Aβ) peptide can bind iron ions at sites Asp (D)1, Glu $(E)_3$, and His $(H)_{6,13,14}$ [16]. However, this peptide has low solubility and a low proportion of iron-binding residues, limiting its ability to purge excess iron in the CSF. Even worse, the $A\beta_{1\text{-}42}$ peptide is presumed to spontaneously generate peptidyl radicals or hydrogen peroxide, which can injure neurons [27, 28].

For more effective iron and radical removal, we combined the metal-pro amino acids histidine (H), glutamic acid (E), and aspartic acid (D), which act as iron ion binders in Aβ to an oligomer; they also combine the polar amino acid tyrosine (Y) and the smallest nonpolar amino acid alanine (A) in the sequence to enhance solubility. By using this approach in cells cultured in an iron-rich medium, we decreased the iron and radical levels in the medium and enhanced cell viability.

When we administered this combination to AD mice, the blood-brain barrier hampered its entry into the brain via ligand-selective endocytosis, thus severely decreasing its therapeutic effects. To solve this problem, intracerebroventricular infusion, CNS drug releasing microchip implantation, pluronic micelles incorporation, and liposome capsule and receptors such as ferritin receptor had been utilized. L-Dopa was reported delivered by a neutral amino acid carrier to the patients with Parkinson's disease, and good curative effect had been obtained [20–23].

For the macromolecular endocytosis ability, the low-density lipoprotein receptor (LDLR) has been utilized to deliver macromolecular drugs, such as proteins, to the brain by being expressed on the BBB [24]. To deliver our designed therapeutic HAYED to AD brains, we synthesized the non-covalent transporter 16ApoE based on the method described by Gobinda [19], linking 16 lysine residues to the LDLR-binding segment of APoE. By mixing this protein with our designed therapeutic peptide mixture HAYED and then cardiac injecting the compound into AD mice, we successfully delivered HAYED into the CSF, and HAYED functioned to remove iron and radicals in the AD brain. In addition to protecting neurons, this protein combination also ameliorated AD symptoms and improved cognition status in AD mice. Hence, our experiment provided a new potential therapeutic drug to ease AD and verified the strategy for administration using receptor-delivering macromolecular agents to the brain to cure brain disease.

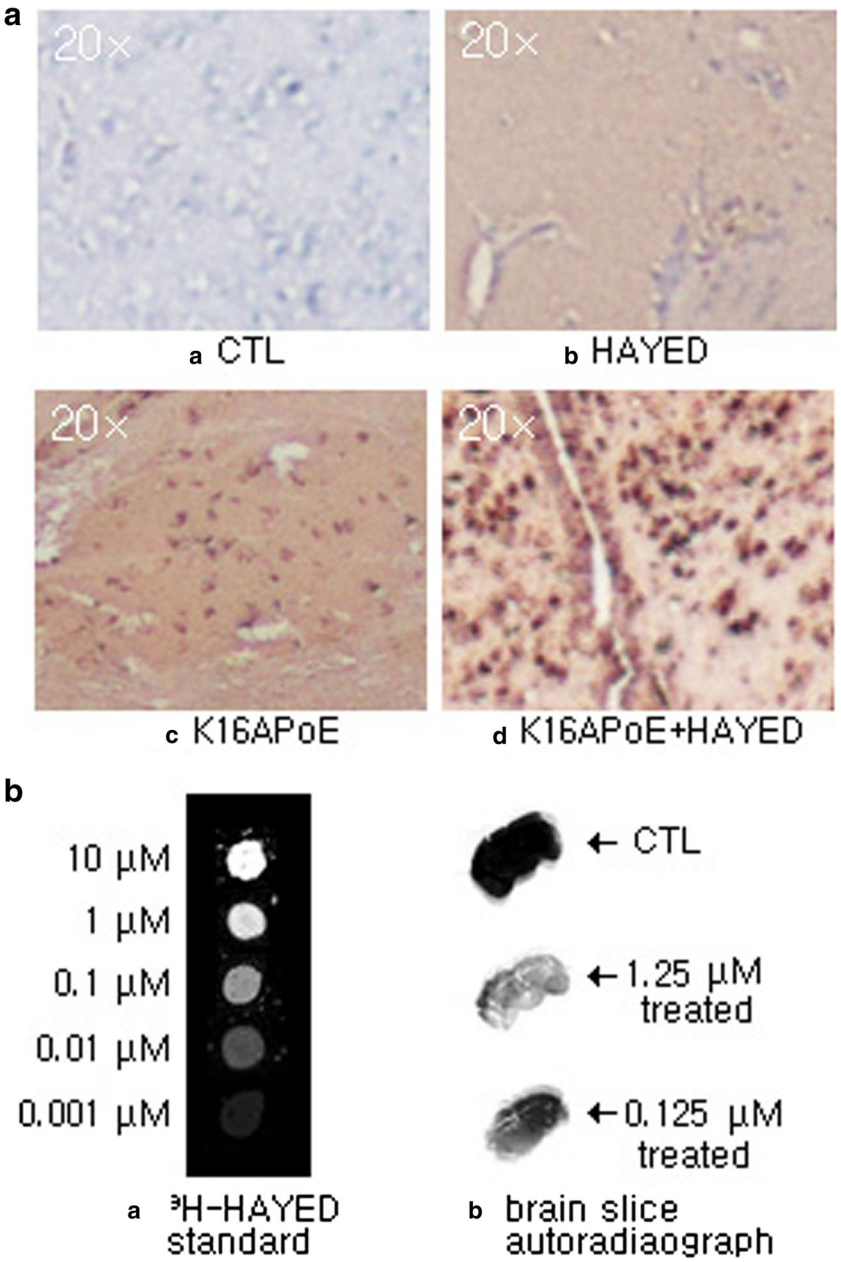

Fig. 4 Synthesized K16APOE enabled HAYED to cross the BBB and enter the brain. **a** Immunohistochemistry shows that the synthesized K16APOE enabled HAYED to cross the BBB and enter the brain. (a) The control brain section exhibited no stained spots. (b) The HAYED-alone treated brain also exhibited no staining, suggesting that HAYED did not enter the brain. (c) In the K16APoE-injected group, the anti-K16APoE serum labeled the section, suggesting that K16APoE entered the brain. (d) In the HAYED-K16APoE mixture-treated brain section, there were scattered brown-stained anti-HAYED spots, suggesting that the synthesized K16APOE enabled HAYED to cross the BBB and enter the brain; **b** ^{3}H-HAYED autoradiography shows the bioavailability of the HAYED penetrated to brain. Two days after the cardiac injection of 200 μl 1.25 μM ^{3}H-HAYED-K16APoE mixture, the concentration of the remnant ^{3}H-HAYED in the brain was about 0.3 μM, which being still active

Conclusion

The synthesized transporter K16APoE can transport the therapeutic HAYED peptide to the brain to remove excess free iron and iron-catalyzed radicals in CSF, thus protecting neurons and improving cognitive status in AD suffers.

Materials and methods

Materials

The amino acid oligomer HAYED, ^{3}H-HAYED (35 μCi/mg), and K16APoE were synthesized and provided by GL Biochem Ltd. (Shanghai, China). $FeCl_3.6H_2O$ was provided by Jingke Chemical Factory (Wuxi, China). The neuroblastoma cell line SH-sy5y was purchased from ATCC (American Type Culture Collection, Manassas, VA, USA). Dulbecco's Modified Eagle's Media (DMEM) and fetal bovine serum (FBS) were purchased from Gibco™ Ltd. The AD model Kunming mice were provided by the Model Animal Research Center of the Chinese Academy of Medical Sciences (MARC, CAMS, Beijing, China).

Amino acid oligomer confirmation

The amino acid oligomers mentioned in the experiment were confirmed by a mass spectrometer (Waters ZQ2000, Milford,

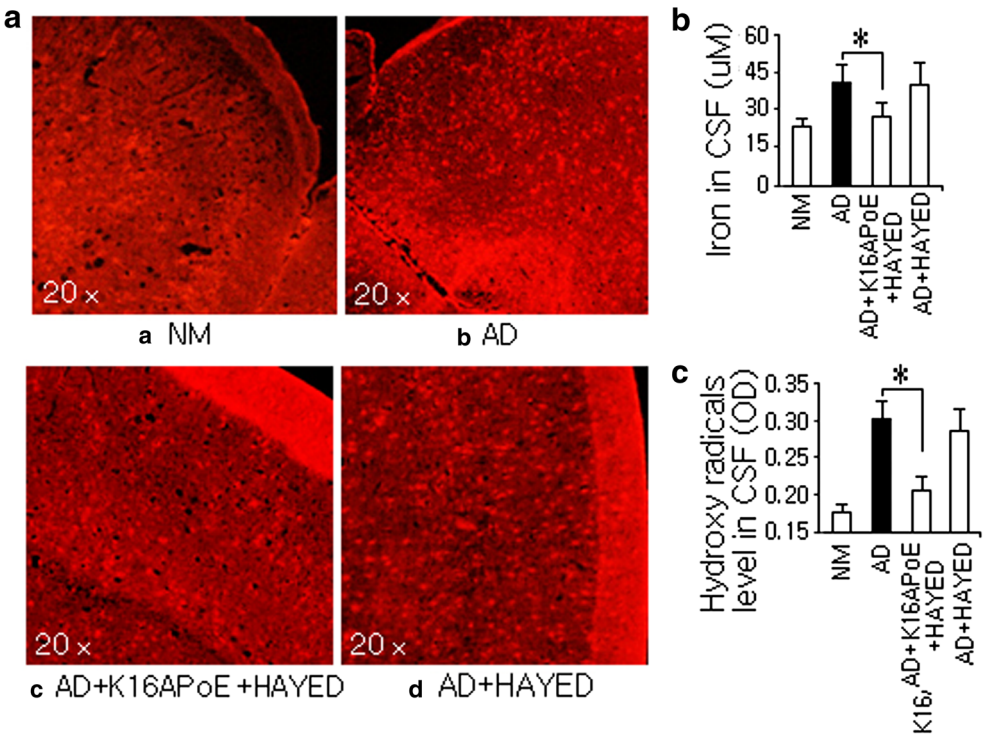

Fig. 5 K16APoE enabled HAYED to enter the brain and scavenge iron and radicals as well as protect neurons. **a** Normal mouse brain. **b** Iron level in cerebrospinal fluid. **c** Hydroxy radical level in cerebrospinal fluid. Without K16APoE, even in the HAYED-injected brain, the iron and hydroxyl radical levels were high, and the necrotic neuron were as numerous as those in the AD mouse. In contrast, when the HAYED was cardiac injected into the mice with K16APoE, the brain iron and hydroxyl radicals decreased; as a result, the number of necrotic neurons was reduced, suggesting that K16APoE enabled the therapeutic HAYED cross the BBB and enter the brain to function in the role of brain protection. $N = 5$; $^*p < 0.05$

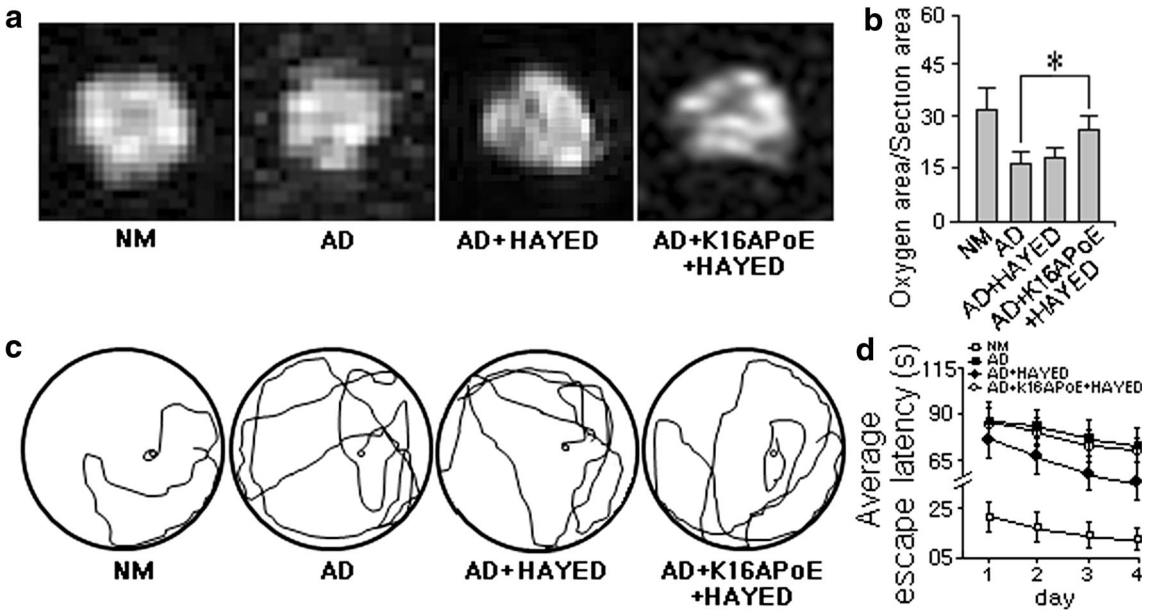

Fig. 6 Cognition assay by fMRI and Morris water maze. fMRI was performed to measure the blood oxygen metabolism level in the brain, and the Morris water maze was adopted to determine the time spent to find the underwater stage. The bright regions in the brain indicate the active blood-oxygen metabolism zones; the wider the region, the more active the brain. **a**, **b** The area of blood oxygen metabolism in the wild-type aged AD mouse occupied approximately 15% of the whole brain, whereas, for the HAYED-K16APoE mixture-treated mouse, the blood oxygen active region occupied approximately 27% of the whole area, which was 1.5 times wider than that of the untreated wild-type aged AD mice and approximately half that of the normal mice. However, if HAYED was not mixed with K16APoE, the level of blood oxygen metabolism was nearly the same as that of the AD mouse, suggesting that without the help of K16APoE, HAYED cannot enter the CSF to function in the role of neuron protection. **c** The distance that the HAYED-K16APoE-treated AD mice swam to find the platform was obviously shorter than that swum by the untreated AD individual. **d** The HAYED-K16APoE compound-treated AD mice spent approximately 59 s on average to swim back to the underwater stage, which was 23 s less than the untreated AD mice. $N = 5$; $^*p < 0.05$

MA, USA) and sequenced by a Procise™ 491 protein sequencer (ABI Companies, Inc., TX, USA) according the manual's instructions.

Infrared spectroscopic analysis of the binding of the peptide to iron atoms

To analyze the binding of the oligomer HAYED to the iron atoms, an infrared spectroscopic analysis was performed. In brief, a 30 μmol dose of the synthesized HAYED oligomer was incubated with 0.5 ml of an $FeCl_3$ solution (50 μM) at 37 °C for 2 h. The air-dried powder was analyzed using an IRPrestige-21 infrared spectrometer (Shimadzu Inc., Kyoto JPN). The changes in the spectral line were considered groups of amino acid residues in the peptide that had been affected by the $FeCl_3$ solution, particularly by the iron atom binding.

HAYED-binding iron assay with X-ray spectrometer and TEM

The synthesized HAYED oligomer powder was dissolved in distilled water (1.25 mM) and then divided into two parts. The first part was used as a control, without iron solution introduction. For the second part, 5 μl of a 0.05 M $FeCl_3 \cdot 6H_2O$ solution were dissolved in 20 μl of HAYED lyosol, and then the mixture was incubated for 1 h at 37 °C. Following that, each share was individually dropped onto a copper mesh supported Formvar film. After negatively staining with 0.2% (*m*/*v*) uranyl acetate (pH 4.5) for 2 min, the dye was sucked out with a filter paper and then air-dried. The samples were finally subjected to a transmission electron microscope (TEM, H7650, Hitachi, Kyoto, JPN) for observation. The iron distributions in the samples were detected using an EMAX X-ray energy spectrometer (Horriba, Kyoto, JPN) equipped on the TEM.

Isothermal titration calorimetry (ITC)

To confirm the affinity between the iron atoms and HAYED, purified HAYED oligomers were exhaustively dialyzed against the ITC buffer (10 mM phosphate, 238 mM NaCl, and 2.7 mM KCl, pH 7.4). Following the dialysis, HAYED oligomers were diluted to 200 μM as measured by OD280 (NanoDrop 1000, Thermo Scientific), and $FeCl_3 \cdot H_2O$ was diluted to 1000 μM. The binding between iron and the HAYED oligomers was measured using a VP-ITC Microcalorimeter (MicroCal, GE Healthcare), and the data were processed using Origin software (OriginLab, Northampton, MA). The $FeCl_3$ solution was transferred to the sample cell, and the syringe was loaded with HAYED solution. The samples were measured at 30 °C, and the system was set to provide a reference power of 10 μcal/s. Thirty 10-μl injections were performed with a 250-s interval between injections. To determine the heat of the ligand dilution, HAYED solution was injected into the ITC buffer utilizing the same parameters as those used in the experimental runs. The heat of the ligand dilution was subtracted from the heat of the binding to generate a binding isotherm that was fit with a one-site binding model using Origin, allowing for the association constant (Ka), enthalpy (ΔH), and entropy (ΔS) of the interaction to be determined. Ka was used to calculate Kd (Kd = 1/Ka). The ITC data were collected in quadruplicates for each sample with independent preparations of $FeCl_3$.

Hydroxyl radical assay

A 2% (*m*/*v*) salicylic acid solution was prepared and maintained at 4 °C. Then, 150 μl of the culture medium or CSF (extracted from the brains of euthanized mice) from each sample was individually mixed with 50 μl of salicylic acid (triple for each). After a 10-min incubation at room temperature, the sample media were centrifuged for 10 min at 10000 rpm. Each supernatant was independently dropped into a well of a 96-well plate, and the light absorption was detected using a microplate reader (Sunrise™, Tecan, Austria) at 450 nm. The OD value was used to determine the hydroxyl radical level in the medium.

Iron content assay

One milliliter of the middle layer of each cultured medium or CSF was dried at 60 °C and then mixed with 1 ml of pure nitric acid. After 2 h of incubation, the mixture was evaluated using a Plasma-coupled chromatograph (ICP, ELAN DRC-e, PerkinElmer Inc., USA) to determine the iron content. Gradient concentration $FeCl_3$ solutions were used as the standard samples.

Brain HAYED bioavailability assay by quantitative autoradiography

After 48 h of cardiac injection of 200 μl ^{3}H-HAYED-K16APoE mixture, the mouse brains were frozen-sectioned to 5 μm coronal slices. Along with a series of freeze air-dried gradient concentration ^{3}H-HAYED-K16APoE mixture droplets on another slide, the brain slices pasted on a glass slide were then placed in an X-ray cassette that contained ^{3}H-sensitive autoradiography film (Leica Inc., Deerfield, IL, USA). Exposed for 2 weeks at room temperature, the autoradiography film was then developed and fixed. Following that, the films were digitized to produce digital images that were 512 × 512 pixels with 256 Gy levels. The tritium activity at each pixel location was used to presenting the bioavailability of the HAYED peptide distributed in the brain; it was determined by comparing the pixel absorbance to a standard curve obtained from digital images of the gradient concentration ^{3}H-HAYED-K16APoE mixture. The freeware program NIH-

Image (written by Wayne Rasband; available by anonymous FTP from zippy.nimh.nih.gov) was used to measure concentration profiles from individual digital images. Local concentrations obtained by this method were in radioactivity units (nCi/mg).

Anti-HAYED/K16APoE immune serum preparation

tBefore the immunohistochemical test, 100 μl of HAYED/K16APoE-physiological saline (0.5 mg/ml) was mixed with 100 μl incomplete Freund adjuvant, and then subcutaneously or intraperitoneally injected into mouse every week. After 2 months, the whole blood of each mouse was extracted, and the serum containing anti-HAYED/K16APoE IgG was isolated and frozen at − 20 °C for future usage.

Immunohistochemical staining

Frozen brain slices were fixed for 12 h with 4% formaldehyde (*v*/*v*), washed three times with 0.1 M phosphate buffer (PBS, pH 7.2), and then blocked with 0.1% BSA/PBS (*m*/*v*). After 1 h, anti-HAYED or anti-K16APoE serum (diluted 1:1000 in PBS) was added to the sections for an overnight incubation at 4 °C. After that, the slices were washed with PBS and covered with HRP-labeled goat-anti-mouse IgG (diluted 1:300 in PBS), followed by 2 h of room temperature incubation. After washing with PBS three times, the samples were irrigated with H_2O_2 and then stained with DAB. After three PBS washes, the samples were covered and observed under a microscope. The spots stained brown were the HAYED or K16APoE positions.

Cell viability assay

The cells in each well were treated with 100 μl of a 1% (*m*/*v*) trypan blue solution for 3 min and then observed under a microscope. The dark-stained cells were considered to be dead. The partially stained cells were considered dying. The ratio of the completely stained cells to the total number of cells in a visual field was considered the mortality rate.

TUNEL assay

High iron-induced cell necrosis in brain tissue was assessed using a TUNEL kit (Order No. E607172, Sangon Biotech Inc. Shanghai, China). In brief, frozen sections (10-μm thickness) were prepared the brain of each mouse, and then the brain slices were placed on slides. After the samples were incubated in Na-HEPES solution for 1 h, they were treated with 10 mM H_2O_2 and 20 mM progesterone. After 1 h, the samples were air-dried; the next day, they were washed in PBS and then permeabilized with 0.1% Triton-X100. Following that, the samples were incubated in the dark at 37 °C for 1 h in TUNEL reaction mixture containing 50 μL terminal deoxynucleotidyl transferase and Dutp. Then, the samples were stained with rhodamine-labeled IgG and analyzed with microscopy. The red fluorescence spots were the necrotic cells in the tissue.

Functional magnetic resonance imaging (fMRI) and Morris water maze assays

Morris water maze and fMRI assays were performed to evaluate the cognitive status of the tested mice. Specifically, the KM mice were divided into the normal, wild-type aged AD model, HAYED alone or HAYED-K16APoE mixture-treated groups. In the HAYED alone or K16APoE-HAYED mixture groups, 1.5 μM HAYED or HAYED-K16APoE mixture (dissolved in phosphate-buffered saline) was cardiac-injected into each mouse weekly. After 1 month of the treatment, all groups of mice underwent a 4-day Morris water maze (a 140-cm diameter circular water tank with a height of 45 cm filled with water made opaque by adding dry milk powder to the water at a temperature of 21–23 °C) assay. The time spent and distance swum to find and return to the underwater platform (15 cm in diameter, 42 cm in height) were recorded to evaluate the individual cognitive status. An fMRI assay was performed using an NMR spectrometer (E40, Flir Inc., USA) at 1.5 T for 30 min after anesthesia. The bright area in the encephalica was used to characterize the oxygen metabolism level in the brain.

Data processing

Data are presented as the means ± SEM of three or more independent experiments, and differences were considered statistically significant at $p < 0.05$ using *t* tests.

Funding information This study was supported by the Public Welfare Technology Research Grant for Zhejiang Social Development [2015C33248], Natural Science Foundation of Zhejiang Province [Y17H160027], Open Object of the Key Laboratory of Shanghai Forensic Medicine [KF1606], Taizhou Science and Technology Program [1501KY32], Taizhou University Research Fund [0104010004], Taizhou University Talent Fostering Fund [2015PY028], and Public Applied Technology Research Project of Zhejiang Province [2015C37081].

Compliance with ethical standards

Conflict of interest The authors declare that they have no conflicts of interest.

References

1. Querfurth HW, LaFerla FM. Alzheimer's disease. N Engl J Med. 2010;362(4):329–44.
2. Thompson CA, Spilsbury K, Hall J, Birks Y, Barnes C, Adamson J. Systematic review of information and support interventions for caregivers of people with dementia. BMC Geriatr. 2007;7:18.

3. Gumienna-Kontecka E, Pyrkosz-Bulska M, (2014). Iron chelating strategies in systemic metal overload, neurodegeneration and cancer, Curr Med Chem. [Epub ahead of print].
4. Hardy J, Allsop D. Amyloid deposition as the central event in the aetiology of Alzheimer's disease. Trends Pharmacol Sci. 1991;12(10):383–8.
5. Mudher A, Lovestone S. Alzheimer's disease-do tauists and baptists finally shake hands? Trends Neurosci. 2002;25(1):22–6.
6. Zou Z, Ma C, Zou R, Cheng L, Wang J, Zhi H, et al. Transitional metals distribution in tissues of transgenic Alzhemier's disease model mice, and the involved roles of AD. Journal of Nanjing Agricultural University. 2007;30(2):116–21. Chinese
7. Liu G, Men P, Perry G, Smith MA. Nanoparticle and iron chelators as a potential novel Alzheimer therapy. Methods Mol Biol. 2010;610:123–44.
8. Kontoghiorghes GJ. New concepts of iron and aluminium chelation therapy with oral L1 (deferiprone) and other chelators. A Rev Anal. 1995;120:845–85.
9. McLachlan DR, Kruck TP, Lukiw WJ, Krishnan SS. Would decreased aluminum ingestion reduce the incidence of Alzheimer's disease? CMAJ. 1991;145:793–804.
10. Crowe A, Morgan EH. Effects of chelators on iron uptake and release by the brain in the rat. Neurochem Res. 1994;19:71–6.
11. Gassen M, Youdim MB. The potential role of iron chelators in the treatment of Parkinson's disease and related neurological disorders. Pharmacol Toxicol. 1997;80:159–66.
12. Bergeron RJ, Brittenham GM. The development of iron chelators for clinical use. CRC; Boca Raton, 1994, 353–371.
13. Galanello R, Campus S. Deferiprone chelation therapy for thalassemia major. Acta Haematol. 2009;122(2–3):155–64.
14. Levy M. Observational Study of Deferiprone (Ferriprox®) in the Treatment of Superficial Siderosis, https://clinicaltrials.gov/ct2/show/NCT01284127.
15. Vivekanandan S, Brender JR, Lee SY, Ramamoorthy A. A partially folded structure of amyloid-beta(1-40) in an aqueous environment. Biochem Biophys Res Commun. 2011;411(2):312–6.
16. Bousejra-ElGarah F, Bijani C, Coppel Y, Faller P, Hureau C. Iron (II) binding to amyloid-β, the Alzheimer's peptide. Inorg Chem. 2011;50(18):9024–30.
17. Atwood CS, Scarpa RC, Huang X, Moir RD, Jones WD, Fairlie DP. Characterization of copper interactions with Alzheimer amyloid beta peptides: identification of an attomolar-affinity copper binding site on amyloid beta1–42. J Neurochem. 2000;75(3):1219–33.
18. Zhang W, Johnson BR, Suri DE, Martinez J, Bjornsson TD. Immunohistochemical demonstration of tissue transglutaminase in amyloid plaques. Acta Neuropathol. 1998;96(4):395–400.
19. Gobinda S, Geoffry LC, Eric M, Teresa D, Thomas M, Wengenack, et al. A carrier for non-covalent delivery of functional Beta-galactosidase and antibodies against amyloid plaques and IgM to the brain. PLoS One. 2001;6(12):e28881.
20. Deane R, Sagare A, Hamm K, Parisi M, LaRue B, Guo H, et al. IgG-assisted age dependent clearance of Alzheimer's amyloid beta peptide by the blood-brain barrier neonatal Fc receptor. J Neurosci. 2005;25:11495–503.
21. Jefferies WA, Brandon MR, Hunt SV, Williams AF, Gatter KC, Mason DY. Transferrin receptor on endothelium of brain capillaries. Nature. 1984;312:162–3.
22. Zlokovic BV, Jovanovic S, Miao W, Samara S, Verma S, Farrell CL. Differential regulation of leptin transport by the choroid plexus and blood-brain barrier and high affinity transport systems for entry into hypothalamus and across the blood-cerebrospinal fluid barrier. Endocrinology. 2000;141:1434–41.
23. Gabathuler R. Approaches to transport therapeutic drugs across the blood–brain barrier to treat brain diseases. Neurobiol Dis. 2010;37:48–57.
24. Spencer BJ, Verma IM. Targeted delivery of proteins across the blood brain barrier. Proc Natl Acad Sci U S A. 2007;104:7594–9.
25. Bush AI. Metal complexing agents as therapies for Alzheimer's disease. Trends in Neurobiol Aging. 2003;25:1031–8.
26. Danielle GS, Roberto C, Kevin JB. The redox chemistry of the Alzheimer's disease amyloid β peptide. Biochim Biophys Acta. 2007;1768:1976–90.
27. Connor JR, Menzies SL, St. Martin SM, Mufson EJ. A histochemical study of iron, transferrin, and ferritin in Alzheimer's disease brains. J Neurosci Res. 1992;31(1:75–83.
28. Lahiri DK, Maloney B. Beyond the signaling effect role of amyloid–β 42 on the processing of AβPP, and its clinical implications. Exp Neurol. 2010;225(1):51–4.